Journal of Fluids and Structures (2002) **16**(5), 627–648
doi:10.1006/jfls.443. available online at http://www.idealibrary.com on IDEAL®

CONTROL OF BLADE FLUTTER USING CASING WITH ACOUSTIC TREATMENT

X. SUN

Department of Jet Propulsion, Beijing University of Aeronautics and Astronautics Beijing, China

AND

S. KAJI

Department of Aeronautics and Astronautics, University of Tokyo, Tokyo, Japan

(Received 8 March 2000; and in final form 25 August 2001)

Control of blade flutter by use of a nonrigid wall may have several advantages compared with the existing method of suppressing blade flutter; but it indeed leads to numerous theoretical problems which have never been clearly elucidated by the existing theories. In the present investigation a new lifting surface model has been suggested based on the application of generalized Green's function theory and double Fourier transformation technique, which is expressed as various upwash integral equations and the corresponding kernel function. In particular, it is found that the change of wall boundary condition not only affects the eigenvalues of the system but also the eigenfunction normalizing factor in comparison with a rigid boundary condition, and it is these variations that finally affect the flow and acoustic field. In addition, the numerical results show that whether a nonrigid wall has positive or negative effect on suppressing blade flutter will mainly depend on what admittance value the wall possesses. It is clear that this conclusion has two implications. One is that there is indeed some possibility for designing a liner for suppressing blade flutter. The second is that modern jet engines using a nonrigid wall or liner to suppress the noise can introduce a detrimental effect on blade flutter stability.

1. INTRODUCTION

DURING THE PAST TWO DECADES, numerous researchers (Bendiksen 1988, 1993; Marshall & Imregun 1996) have investigated the feasibility of suppressing or controlling flutter in turbomachinery rotors. Most of the proposed methods fall into three main categories: (i) mistuning, (ii) aeroelastic tailoring and (iii) dry friction damping or mode shape control. In addition to the above methods which have received great attention, a novel way of controlling blade flutter by use of a nonrigid wall or soft wall was also suggested by Watanabe and Kaji (1984) and Namba *et al.* (1984), respectively. Their research objective was to try to find flutter-suppressing liners. For this purpose Watanabe & Kaji (1984) used a three-dimensional semi-actuator disk model to evaluate the effects of a nonrigid wall on the aerodynamic damping which is a key factor in determining whether the blade flutters or not. Namba *et al.* (1984) treated the nonrigid wall as unsteady equivalent surface mass source singularities developed by Namba & Fukushige (1982) and then obtained numerical results by solving three-dimensional linearized Euler equations under a hard

0889-9746/02/050627 + 22 $35.00/0

wall condition. Their results all show that a nonrigid wall can influence the unsteady pressure distribution and the aeroelastic stability of blades, which depends on the aerodynamic and geometrical parameters of the cascade and the range of the acoustic admittance value of the wall. However, no further work has been done in this direction since then.

In fact, if this idea is found to be feasible, there will be at least two advantages. On the one hand, it can be shown that the application of flutter-suppressing liners will not cause any apparent aerodynamic loss or weight penalty compared with the existing methods. On the other hand, as is well known, in recent years there have been studies on the active control of isolated airfoil flutter, using loudspeakers or piezoelectric materials as the actuators. From the viewpoint of application, it is very impractical to directly apply the same technology as that in the active control of isolated airfoil flutter to the rotating blade in compressors. So, a new approach is required for the active control of blade flutter in compressors. However, for a given liner with honeycomb structure which is widely used to suppress the noise generated by jet engines, the impedance is in general fixed. So, there would be no possibility for active control. However, it has been found that there is a liner with adjustable impedance which consists of a perforated plate and the bias flow through the holes (Bechert 1980; Howe 1979*a*,*b*). Recent fundamental experimental and theoretical work (Dowling & Hughes 1992; Hughes & Dowling 1990; Jing & Sun 1999) has shown that such liner would be a good prospect for many applications (Zhao & Sun 1999). There is reason, therefore, to believe, assuming the availability of flutter-suppressing liner with adjustable impedance, that it would be possible to realize the active control of compressor blade flutter. To achieve this goal, considerable research on the following items is needed.

First, the essence of this problem is actually to change the aerodynamic damping of a blade through the variation of the wall boundary condition. Hence, the accurate unsteady aerodynamic model for a nonrigid wall condition is one problem of interest. However, it is noted that the existing lifting surface theories (Namba 1977; Lordi & Homicz 1981; Shulten 1984) for unsteady aerodynamics and aeroacoustics of turbomachines, which in general are expressed in the form of an upwash integral equation, have all utilized the orthogonality of the eigenfunctions under the boundary condition of a hard wall. However, Tester (1972) and Zorumski (1974) have shown the eigenfunctions no longer exhibit the orthogonality property for a lined duct containing uniform mean flow. In fact, to the authors' best knowledge, under the condition of a nonrigid wall nobody has given the upwash integral equation for unsteady aerodynamics and aeroacoustics of turbomachines up to now. On the other hand, it is reasonable to believe that the upwash integral equation can be obtained so long as the corresponding Green's function is given. Hence, the core of the problem is how to derive a correct Green's function under a soft wall condition. This actually introduces a problem which has not been fully resolved even for the purely acoustic problem (Tester 1972; Sijtsma 1995). There is very limited work on this subject. The first attempt was carried out by Tester (1972), who derived a Green's function for a duct with an arbitrary locally reacting admittance on one wall by using a fundamental method given by Brekhovskikh (1960). Also, due to the limitations of the methods used by him, the assumption that the distance to the wall boundary from either observer point or source point is larger than half a wavelength has to be imposed on the boundary condition. However, it is worth noting that Zorumski (1974) presented an important clue towards the derivation of Green's function for a lined duct, in which the boundary condition is directly coupled with the basic equations by using Fourier transforms. Besides, this work has actually verified there is a solution which consists of non-orthogonal eigenfunctions. In fact, the mode-matching approach widely used in duct

acoustics is based on this theoretical frame. Hence, what is done in the present study is to find such solution by using an effective mathematical tool.

Secondly, it has been known that the boundary condition of a nonrigid wall influences the flow field or acoustic field theoretically by introducing the variations of the eigenvalues. For a lined duct, the eigenvalues are generally complex. Thus the calculation of the accurate eigenvalues has been a subject that has received considerable attention (Ko 1973; Eversman 1975, 1977). In addition, for the present problem the eigenvalue equation describing the boundary condition differs from that used in pure duct acoustics due to the characteristics of a moving sound source. Hence, the derivation of the eigenvalue equation and an effective approach for the calculations of the eigenvalues is a relevant problem.

Finally, the boundary condition of a nonrigid wall is described by acoustic impedance or admittance. Under the condition of grazing flow and high sound intensity, development of a reasonable acoustic model of the wall is an important issue.

In the present study, the emphasis is placed on the first two problems. First, the double Fourier transform technique is applied to obtain the Green's function for a duct with an arbitrary locally reacting admittance on one wall. Subsequently, an upwash integral equation is derived by using generalized Green's function theory and solving three-dimensional Euler equations for a given cascade geometry. It can be shown that by letting the admittance of the wall become zero the results can be reduced to those obtained by previous investigators for the hard wall case. On the other hand, the eigenvalue equation describing the boundary condition has been transformed into a nonlinear ordinary equation, which is then solved by a fourth-order Runge–Kutta scheme. The computational results of the eigenvalues show very good agreement with the existing results for a nonrigid wall. Based on the above verification, the calculation is then extended to investigate the effect of a nonrigid wall on the flow of a stator and rotor blade row. It is found that the change of wall admittance will lead to remarkable effects on both lift, moment coefficient and aeroelastic stability of a blade row. Finally, concluding remarks are given on the basis of the present theory and the corresponding numerical simulation.

2. FLOW MODEL

2.1. Basic Equations

The cascade flow model used in this analysis is shown in Figure 1, all variables being physical or dimensional ones. Later scale lengths will be taken with respect to the semichord b for convenience. In addition, the following assumptions are made: (i) the system is three-dimensional, with a mean flow between two infinite parallel plates, as shown in Figure 1; especially the lower plate (hub side) is assumed rigid while the upper plate (tip side) is assumed to have a finite acoustic impedance; (ii) the blades are flat plates of negligible thickness; (iii) the mean angle of incidence is zero; there is no steady blade loading and the mainstream flow passes through the cascade undeflected; (iv) all perturbations from the uniform mean flow are small, so that the flow equations may be linearized and the principle of superposition applied to the solutions obtained; (v) the unsteady blade loading at the trailing edge is finite; this is the statement of the Kutta–Joukowski condition for unsteady flow; (vi) the flow is subsonic.

In addition to the above assumptions, it has been noted that, when the wall admittance has a positive imaginary part, an unsteady mode will be triggered, which is related to Helmholtz instability waves (Tester 1972; Rienstra 1986). In the present analysis, the effect of unstable surface modes will be ignored. So, the perturbation pressure p induced by the

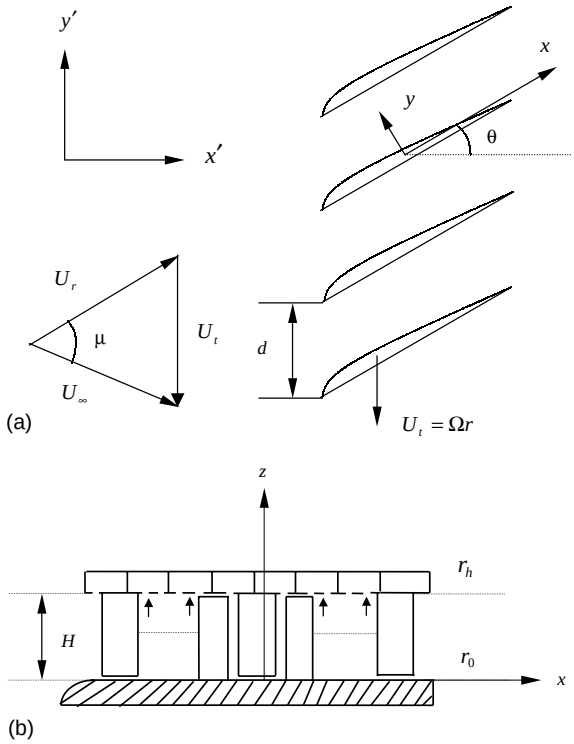

Figure 1. Schematic of flow model.

motion of the blade is then governed by the wave equation

$$(1 - M_r^2)\frac{\partial^2 p}{\partial x^2} + \frac{\partial^2 p}{\partial y^2} + \frac{\partial^2 p}{\partial z^2} - \frac{1}{a_0^2}\frac{\partial^2 p}{\partial t^2} - \frac{2M_r}{a_0}\frac{\partial^2 p}{\partial x \partial t} = 0, \tag{1}$$

where M_r is the mean flow Mach number in x-direction as shown in Figure 1, p is the fluctuating pressure, a_0 is the velocity of sound.

The boundary condition is assumed to satisfy

$$\begin{aligned} &\frac{\partial p}{\partial n} + b(\mathbf{y})p = a(\mathbf{y}, \tau) \quad \text{if } \mathbf{y} \text{ on the tip side of duct,} \\ &\frac{\partial p}{\partial n} = 0 \qquad\qquad\qquad \text{if } \mathbf{y} \text{ on the hub side of duct.} \end{aligned} \tag{2}$$

The Green's function of equation (1) satisfies

$$(1 - M_r^2)\frac{\partial^2 G}{\partial x_0^2} + \frac{\partial^2 G}{\partial y_0^2} + \frac{\partial^2 G}{\partial z_0^2} - \frac{1}{a_0^2}\frac{\partial^2 G}{\partial \tau^2} - \frac{2M_r}{a_0}\frac{\partial^2 G}{\partial x \partial \tau} = -\delta(t - \tau)\delta(\mathbf{x} - \mathbf{y}). \tag{3}$$

The corresponding boundary condition is

$$\begin{aligned} &\frac{\partial G}{\partial n} + b(\mathbf{y})G = 0 \quad \text{if } \mathbf{y} \text{ on the tip side of duct,} \\ &\frac{\partial G}{\partial n} = 0 \qquad\qquad\qquad \text{if } \mathbf{y} \text{ on the hub side of the duct.} \end{aligned} \tag{4}$$

According to the generalized Green's function theory (Goldstein 1976), the solution of equation (1) will be able to be expressed as

$$p(\mathbf{x}, t) = \int_{-T}^{T} d\tau \int_{A} \left[G\left(\frac{\partial}{\partial n} + \frac{V_n}{a_0^2}\frac{D_0}{D\tau}\right) p(\mathbf{y}, \tau), - p(\mathbf{y}, \tau)\left(\frac{\partial}{\partial n} + \frac{V_n}{a_0^2}\frac{D_0}{D\tau}\right) G(\mathbf{y}, \tau|\mathbf{x}, t)\right] \mathrm{d}S(\mathbf{y}). \tag{5}$$

2.2. Solution of Green's Function

Suppose G_ω represents the Fourier transforms of Green's Function in equation (3). Introducing the coordinate transforms $\xi = x/b$, $\eta = y\beta_r/b$, $\zeta = z\beta_r/b$ and then substituting $G_\omega = G'_\omega e^{iKM_r\xi}$ into equation (3) yields (Morse & Feshbach 1953)

$$G'_\omega = A\cos K_q\zeta_0 + B\sin K_q\zeta_0 - \frac{e^{-i[\omega t+(\alpha+KM_r)\xi+\beta\eta]}}{bK_q}\begin{cases} \cos K_q\zeta_0 \sin K_q\zeta, & \zeta_0 \leqslant \zeta \\ \cos K_q\zeta \sin K_q\zeta_0, & \zeta_0 \geqslant \zeta, \end{cases} \tag{6}$$

where

$$K = \frac{\omega b}{a_0\beta_r^2}, \tag{7}$$

$$\beta_r = \sqrt{1 - M_r^2}. \tag{8}$$

To determine the constants A and B, the concrete expression of the boundary condition defined in equation (2) is needed.

2.3. Boundary Condition for a Lined Duct

The liner can be modelled by a vortex sheet separating the uniform mean flow region within the duct from the no-flow region in the liner (Ko 1973). The impedance boundary condition is then applied on the no-flow side. The two regions are coupled by matching the pressure p and the particle displacement ξ_p. From equation (6), it can be assumed that the displacement be of the form

$$\xi_p = \xi_{pa} e^{i[\omega\tau+(\alpha+KM_r)\xi_0+\beta\eta_0]}. \tag{9}$$

However, if the relative movement between the wall and the blades is considered, laboratory-fixed coordinates will have to be used. So, the following transformations are needed:

$$x = x'\cos\theta + (y' + \Omega r_m\tau)\sin\theta,$$

$$y = -x'\sin\theta + (y' + \Omega r_m\tau)\cos\theta,$$

$$z = z', \tag{10}$$

where Ω and r_m represent the rotating speed of the rotor and the mean radius of the rotor, respectively.

Substituting equation (10) into equation (9) yields

$$\xi_p = \xi_{pa} e^{i(\omega'\tau+\alpha' x'+\beta' y')}, \tag{11}$$

where

$$\alpha' = \frac{\alpha + KM_r}{b}\cos\theta, \tag{12}$$

$$-\beta\frac{\beta_r}{b}\sin\theta, \beta' = \frac{\alpha + KM_r}{b}\sin\theta + \beta\frac{\beta_r}{b}\cos\theta, \tag{13}$$

$$\omega' = \omega + (\beta' r_m)\Omega. \tag{14}$$

With the pressure and displacement matching conditions on both sides of the liner (Ko 1973), it can be shown that

$$\frac{\beta_r}{b}\frac{\partial G_\omega}{\partial\zeta_0} + \mathrm{i}\beta_a k_0'(1 + \frac{\alpha'}{k_0'}M_x - \frac{\beta'}{k_0'}M_y)^2 G_\omega = 0, \tag{15}$$

where

$$k_0' = \frac{\omega'}{a_0} = \frac{\omega + (\beta' r_m)\Omega}{a_0}. \tag{16}$$

2.4. Determination of Green's Function

Let

$$\Delta_{\zeta_0}(G_\omega) = \frac{\beta_r}{b}\frac{\partial G_\omega}{\partial\zeta_0} + \mathrm{i}\beta_a k_0'\left(1 + \frac{\alpha'}{k_0'}M_x - \frac{\beta'}{k_0'}M_y\right)^2 G_\omega\Big|_{\zeta_0 = h} = 0. \tag{17}$$

Since

$$\left.\frac{\partial G}{\partial\zeta_0}\right|_{\zeta_0=0} = 0, \tag{18}$$

it can be verified that

$$G = \frac{1}{(2\pi)^3}\int_{-\infty}^{+\infty}\int_{-\infty}^{+\infty}\int_{-\infty}^{+\infty}\left[\frac{\cos K_q\zeta\cos K_q\zeta_0\Delta_h(\sin K_q\zeta_0)}{bK_q\Delta_h(\cos K_q\zeta_0)}\right.$$
$$\left. - \frac{1}{bK_q}\begin{Bmatrix}\cos K_q\zeta_0\sin K_q\zeta, & \zeta_0 \leqslant \zeta\\ \cos K_q\zeta\sin K_q\zeta_0, & \zeta_0 \geqslant \zeta\end{Bmatrix}\mathrm{e}^{\mathrm{i}\omega(\tau-t)+i(\alpha+KM_x)(\xi_0-\xi)+i\beta(\eta_0-\eta)}\,\mathrm{d}\alpha\,\mathrm{d}\beta\,\mathrm{d}\omega. \right. \tag{19}$$

2.5. Derivation of Integral Equation

According to the boundary condition described in equation (17), it can be shown that the contribution from both upper and lower walls to the sound pressure at any point of the space surrounded by the walls will be zero. So, the only remaining contribution to sound pressure production is related to the blade rows. Under such conditions, it can further be shown that equation (5) will become

$$p(\mathbf{x}, t) = \int_{-T}^{T}\mathrm{d}\tau\int_{A_{db}}\left(-p\frac{\partial G}{\partial n}\right)\mathrm{d}S(\mathbf{y}), \tag{20}$$

where A_{db} is the periphery of a blade which consists of the upper surface and the lower surface of a blade. Besides, $\mathbf{n}$ is the normal to the surface A_{db} directed into the blade.

Let

$$\Delta p(\xi_0, \zeta_0, \tau) = p^-(\xi_0, \zeta_0, \tau) - p^+(\xi_0, \zeta_0, \tau), \tag{21}$$

where Δp is the pressure difference between the lower and upper surface of a blade.

Assume the blade force changes with time dependence $e^{(i\omega_b \tau)}$, i.e.

$$\Delta p(\xi_0, \zeta_0, \tau) = \Delta \bar{p}(\xi_0, \zeta_0) e^{i\omega_b \tau}; \tag{22}$$

hence

$$p(\mathbf{x}, t) = -\int_{-T}^{T} d\tau \int_{A_b} \Delta p(\xi_0, \zeta_0, \tau) \left(\frac{\beta_r}{b}\right) \frac{\partial G}{\partial \eta_0} dS(\mathbf{y}), \tag{23}$$

where A_b is the upper surface or the lower surface of a blade.

The theory of residues can be used to evaluate the inverse transforms of equation (23). In fact, if let $\Delta_h \cos K_q \zeta_0 = 0$, the poles exist in the β-plane, which are, respectively,

$$\beta = \pm \sqrt{K_b^2 - \alpha^2 - K_q^2}; \tag{24}$$

then, if $\zeta_0 - \zeta > 0$, a contour which circles the upper half of the β-plane is used and, if $\zeta_0 - \zeta < 0$, a contour circling the lower half is used. Hence, it can be further shown that

$$K_q \frac{\partial \Delta_h(\cos K_q \zeta_0)}{\partial \beta} = 2\beta \frac{\beta_r K_q h}{b \cos K_q h} \left[\frac{1}{2}\left(1 + \frac{{}_q h}{2K_q h}\right) + \Lambda_1(\alpha, \beta) + \Lambda_2(\alpha, \beta)\right], \tag{25}$$

where

$$\Lambda_1(\alpha, \beta) = -\frac{i\beta_a M_r}{\alpha h \beta_r}\left(1 + \frac{\alpha'}{k_0'} M_x - \frac{\beta'}{k_0'} M_y\right) \cos^2 K_q h, \tag{26}$$

$$\Lambda_2(\alpha, \beta) = \frac{i\beta_a M_t}{2\beta_r h}\left(1 + \frac{\alpha'}{k_0'} M_x - \frac{\beta'}{k_0'} M_y r\right)^2 \left(\frac{\sin\theta}{\alpha} - \frac{\beta_r \cos\theta}{\beta}\right) \cos^2 K_q h, \tag{27}$$

and

$$\Delta_h(\sin K_q \zeta_0) = \frac{\beta_r K_q}{b \cos K_q h}. \tag{28}$$

So, equation (23) becomes

$$\begin{aligned} p(\mathbf{x}, t) = & -\operatorname{sgn}(\eta - \eta_0) \frac{\beta_r}{4\pi b^2 h} \int_{A_b} \int_{-\infty}^{+\infty} \Delta \bar{p}(\xi_0, \zeta_0) \\ & \times \sum_{q=1}^{+\infty} \left[\frac{\cos K_q \zeta \cos K_q \zeta_0}{\Lambda^{\pm}}\right. \\ & \left. \times e^{i\omega_b t - i(\alpha - K_b M_r)(\xi - \xi_0) - i\sqrt{K_b^2 - \alpha^2 - K_q^2}|\eta - \eta_0|}\right] d\alpha \, dS, \end{aligned} \tag{29}$$

where

$$\operatorname{sgn}(x) = \begin{cases} 1, & x > 0, \\ -1, & x < 0, \end{cases} \tag{30}$$

$$\Lambda^{\pm} = \left[\frac{1}{2}\left(1 + \frac{{}_q h}{2K_q h}\right) + \Lambda_1(\alpha, \beta^{\pm}) + \Lambda_2(\alpha, \beta^{\pm})\right], \tag{31}$$

$$\beta^- = -\sqrt{K_b^2 - \alpha^2 - K_q^2}, \tag{32}$$

$$\beta^+ = \sqrt{K_b^2 - \alpha^2 - K_q^2}. \tag{33}$$

Let

$$\bar{p} = -\operatorname{sgn}(\eta - \eta_0)\frac{\beta_r}{4\pi b^2 h}\int_{A_b}\int_{-\infty}^{+\infty}\Delta\bar{p}(\xi_0,\zeta_0)\sum_{q=1}^{+\infty}\left[\frac{\cos K_q\zeta\cos K_q\zeta_0}{\Lambda^{\pm}}\right.$$
$$\left.\times\, \mathrm{e}^{-\mathrm{i}(\alpha - K_b M_r)(\xi-\xi_0)-\mathrm{i}\sqrt{K_b^2-\alpha^2-K_q^2}|\eta-\eta_0|}\right]\mathrm{d}\alpha\,\mathrm{d}S. \tag{34}$$

As shown in Figure 1

$$\xi_{0m} = \xi_0 + mh_1, \quad m = 0, \pm 1, \pm 2, \cdots, \tag{35}$$

$$\eta_{0m} = mh_2\beta_r, m = 0, \pm 1, \pm 2, \cdots;$$

so, for the mth blade,

$$\bar{p}_m = -\operatorname{sgn}(\eta_m)\frac{\beta_r}{4\pi b^2 h}\int_{A_b}\int_{-\infty}^{+\infty}\sum_{q=1}^{+\infty}\frac{\cos K_q\zeta\cos K_q\zeta_0}{\Lambda^{\pm}}$$
$$\times\,\Delta\bar{p}_m(\xi_{0m},\zeta_{0m})\mathrm{e}^{-\mathrm{i}(\alpha-K_bM_r)[\xi-(\xi_0+mh_1)]-\mathrm{i}\sqrt{K_b^2-\alpha^2-K_q^2}|\eta-mh_2\beta_r|}\,\mathrm{d}\alpha\,\mathrm{d}S, \tag{36}$$

where

$$\eta_m = \eta - mh_2\beta_r. \tag{37}$$

Assume

$$\Delta\bar{p}_m(\xi_{0m},\zeta_{0m}) = \Delta\bar{p}_0(\xi_0,\zeta_0)\mathrm{e}^{\mathrm{i}m\sigma}, \tag{38}$$

where σ is called the interblade phase angle. if the complete solution to equation (1) is expressed simply as a sum over all blades of function $\bar{p}_m$, then

$$\bar{p} = \sum_{m=-\infty}^{m=\infty}\bar{p}_m, \tag{39}$$

and

$$\bar{p} = -\frac{\beta_r}{4\pi b^2 h}\int_{-\infty}^{+\infty}\Delta\bar{p}_0(\xi_0,\zeta_0)\sum_{q=1}^{+\infty}\left[\frac{\cos K_q\zeta\cos K_q\zeta_0}{\Lambda^{\pm}}\right.$$
$$\left.\times\sum_{m=-\infty}^{m=\infty}\operatorname{sgn}(\eta_m)\mathrm{e}^{\mathrm{i}m\sigma-\mathrm{i}(\alpha-K_bM_r)[\xi-(\xi_0+mh_1)]-\mathrm{i}\sqrt{K_b^2-\alpha^2-K_q^2}|\eta-mh_2\beta_r|}\right]\mathrm{d}\alpha. \tag{40}$$

The corresponding upwash integral equation can therefore written as

$$\frac{\bar{v}(\xi,\eta,\zeta)}{U_r} = \int_0^1\int_{-1}^1 f(\xi_0,\zeta_0)K(\xi-\xi_0,\eta,\zeta|\zeta_0)\,\mathrm{d}\xi_0\,\mathrm{d}\zeta_0, \tag{41}$$

where

$$f(\xi_0,\zeta_0) = \frac{\Delta\bar{p}_0(\xi_0,\zeta_0)}{\rho_0 U_r^2}, \tag{42}$$

$$K(\xi-\xi_0,\eta,\zeta|\zeta_0)=\frac{\mathrm{i}\beta_r}{4\pi}\frac{\partial}{\partial\eta}\int_{-\infty}^{+\infty}\sum_{q=1}^{+\infty}\left[\frac{\cos K_q\zeta\cos K_q\zeta_0}{\Lambda^{\pm}\left(\alpha-\dfrac{K_b}{M_r}\right)}\right.$$
$$\left.\times\sum_{m=-\infty}^{m=\infty}\operatorname{sgn}(\eta_m)\mathrm{e}^{\mathrm{i}m\sigma-\mathrm{i}(\alpha-K_bM_r)[\xi-(\xi_0+mh_1)]-\mathrm{i}\sqrt{K_b^2-\alpha^2-K_q^2}|\eta-mh_2\beta_r|}\right]\mathrm{d}\alpha. \tag{43}$$

By letting $\eta\to 0$, an integral equation for the pressure across the 0th blade in terms of the known upwash velocity on the blade surface can be expressed as

$$\frac{\bar{v}(\xi,0,\zeta)}{U_r}=\int_0^1\int^1 -1f\,(\xi_0,\zeta_0)K_0(\xi-\xi_0,\zeta|\zeta_0)\,\mathrm{d}\xi_0\,\mathrm{d}\zeta_0, \tag{44}$$

where

$$K_0(\xi-\xi_0,\zeta|\zeta_0)=\lim_{\eta\to 0}K_0(\xi-\xi_0,\quad\eta,\quad\zeta|\zeta_0). \tag{45}$$

It can further be shown that

$$K(\xi-\xi_0,\zeta|\zeta_0)$$
$$=\frac{i\beta_r}{4\pi}\lim_{\eta\to 0}\frac{\partial}{\partial\eta}\int_{-\infty}^{+\infty}\sum_{q=1}^{+\infty}\frac{\cos K_q\zeta\cos K_q\zeta_0\mathrm{e}^{-\mathrm{i}(\alpha-K_bM_r)(\xi-\xi_0)}}{\left(\alpha-\dfrac{K_b}{M_r}\right)}$$
$$\times\frac{1}{2i}\left[\frac{\mathrm{e}^{\mathrm{i}\sqrt{K^2-\alpha^2-K_q^2}\eta}\mathrm{e}^{i/2\Delta_-}}{\Lambda^-\sin\frac{1}{2}\Delta_-}+\frac{\mathrm{e}^{-\mathrm{i}\sqrt{K^2-\alpha^2-K_q^2}\eta}\mathrm{e}^{i/2\Delta_+}}{\Lambda^+\sin\frac{1}{2}\Delta_+}\right]\mathrm{d}\alpha, \tag{46}$$

where

$$\Delta_-=(\Gamma+h_1\alpha)+h_2\beta_r\beta^-, \tag{47}$$

$$\Delta_+=(\Gamma+h_1\alpha)+h_2\beta_r\beta^+, \tag{48}$$

$$\Gamma=\sigma-K_bM_rh_1. \tag{49}$$

At first glance it might appear that the integrand in this expression possesses branch points due to the appearance of the radical $\sqrt{K_b^2-\alpha^2-K_q^2}$. However, it can easily be verified by replacing $\sqrt{K_b^2-\alpha^2-K_q^2}$ by $-\sqrt{K_b^2-\alpha^2-K_q^2}$ that this function depends only on its square so that the branch points are therefore "cancelled" and the integrand possesses only poles of the integrand at $\alpha_v=K_b/M_r$ and at the points where $\Delta_{\pm}=2n\pi$ for $n=0,\pm1,\pm2,\ldots$. However, it follows from equations (47) and (48) that the latter points are determined by

$$\alpha_n^{\pm}=-\frac{\Gamma_nh_1}{d^2}\pm\frac{\beta_rh_2}{d}\sqrt{K_b^2-K_q^2-\left(\frac{\Gamma_n}{d}\right)^2}, \tag{50}$$

where

$$\Gamma_n=\Gamma-2n\pi,\ \text{for } n=0,\pm1,\pm2,\cdots, \tag{51}$$

$$d=\sqrt{h_1^2+h_2^2\beta_r^2}. \tag{52}$$

When $\xi_0 - \xi < 0$, the contour must be closed in the lower half of the α-plane and when $\xi_0 - \xi > 0$ in the upper plane. Hence, upon evaluating the residues it can be shown that for the vortex wave propagating downstream ($\xi_0 - \xi < 0$)

$$\alpha_v = \frac{K_b}{M_r}. \tag{53}$$

The corresponding kernel function can be expressed as

$$K(\xi - \xi_0, \zeta|\zeta_0) = \frac{\beta_r}{2} \sum_{q=1}^{+\infty} \frac{\cos K_{qv}\zeta \cos K_{qv}\zeta_0}{\Lambda_v} \frac{\beta_v \sin(h_2\beta_r\beta_v) e^{-i(\beta_r^2 K_b/M_r)(\xi-\xi_0)}}{\cos(h_2\beta_r\beta_v) - \cos(\Gamma + \alpha_v h_1)}, \tag{54}$$

where

$$\beta_v = \sqrt{K_b^2 - \alpha_v^2 - K_{qv}^2}.$$

Since the wavelength of the pressure wave and the vortex wave are different from each other, it can be assumed that vortex wave will not be influenced by the wall admittance like the pressure wave. Because of this it can be shown that

$$K_{qv} = \frac{\pi(q-1)}{h} = \frac{\pi(q-1)b}{H\beta_r},\ q = 1, 2, 3, \ \ldots, \tag{55}$$

$$\Lambda_v = \begin{cases} 1, & q = 1, \\ 0.5, & q \neq 1, \end{cases} \tag{56}$$

(i) for the downstream pressure wave ($\xi_0 - \xi < 0$), the kernel function is

$$\begin{aligned} K(\xi - \xi_0, \zeta|\zeta_0) = {} & \frac{\beta_r}{2} \sum_{q=1}^{+\infty} \frac{\cos K_{qv}\zeta \cos K_{qv}\zeta_0}{\Lambda_v} \frac{\beta_v \sin(h_2\beta_r\beta_v) e^{-i(\beta_r^2 K_b/M_r)(\xi-\xi_0)}}{\cos(h_2\beta_r\beta_v) - \cos(\Gamma + \alpha_v h_1)} \\ & + \frac{\beta_r^2 h_2}{2d^2} \sum_{n=-\infty}^{+\infty} \sum_{q=1}^{+\infty} \frac{\cos K_q\zeta \cos K_q\zeta_0}{\Lambda(\alpha_n^+, \beta_n^-)} \frac{(K_b^2 - \alpha_n^{+^2} - K_q^2) e^{-i(\alpha_n^+ - K_b M_r)(\xi-\xi_0)}}{(\alpha_n^+ + \Gamma_n h_1/d^2)(\alpha_n^+ - K_b/M_r)}, \end{aligned} \tag{57}$$

where

$$\Lambda(\alpha_n^+, \beta_n^-) = \left[\frac{1}{2}\left(1 + \frac{\sin 2K_q h}{2K_q h}\right) + \Lambda_1(\alpha_n^+, \beta_n^-) + \Lambda_2(\alpha_n^+, \beta_n^-)\right], \tag{58}$$

$$\Lambda_1(\alpha_n^+, \beta_n^-) = -\frac{i\beta_a M_r}{\alpha_n^+ h \beta_r}\left(1 + \frac{\alpha_n^{+'}}{k_0'} M_x - \frac{\beta_n^{-'}}{k_0'} M_y\right) \cos^2 K_q h, \tag{59}$$

$$\Lambda_2(\alpha_n^+, \beta_n^-) = \frac{i\beta_a M_t}{2\beta_r h}\left(1 + \frac{\alpha_n^{+'}}{k_0'} M_x - \frac{\beta_n^{-'}}{k_0'} M_y\right)^2 \left(\frac{\sin\theta}{\alpha_n^+} - \frac{\beta_r \cos\theta}{\beta_n^-}\right) \cos^2 K_q h, \tag{60}$$

$$\alpha_n^+ = -\frac{\Gamma_n h_1}{d^2} + \frac{\beta_r h_2}{d}\sqrt{K_b^2 - K_q^2 - \left(\frac{\Gamma_n}{d}\right)^2}, \tag{61}$$

$$\beta_n^- = -\frac{\Gamma_n h_2 \beta_r}{d^2} - \frac{h_1}{d}\sqrt{K_b^2 - K_q^2 - \left(\frac{\Gamma_n}{d}\right)^2}, \tag{62}$$

$$\alpha_n^{+'} = \frac{1}{\beta_0^2}\left[-M_x K_t + \sqrt{K_t^2 - \beta_0^2\left[(\beta_n^-)^2 + K_q^2\right]}\right], \tag{63}$$

$$K_t = k_b' - \frac{(\sigma - 2\pi n)M_y}{d'}, \tag{64}$$

$$k_b' = k_b + \frac{(\sigma - 2\pi n)M_t}{d'}, \tag{65}$$

$$\beta_n^{-'} = -\frac{\sigma - 2\pi n}{d'}, \tag{66}$$

$$d' = b\sqrt{h_1^2 + h_2^2}, \tag{67}$$

$$K_q' = \frac{\beta_r}{b} K_q, \tag{68}$$

for the upstream pressure wave ($\xi_0 - \xi > 0$), the kernel function is

$$K(\xi - \xi_0, \zeta|\zeta_0) = \frac{\beta_r^2 h_2}{2d^2} \sum_{n=-\infty}^{+\infty} \sum_{q=1}^{+\infty} \frac{\cos K_q \zeta \cos K_q \zeta_0}{\Lambda(\alpha_n^-, \beta_n^+)} \frac{(K_b^2 - \alpha_n^- 2 - K_q^2)\mathrm{e}^{-\mathrm{i}(\alpha_n^- - K_b M_r)(\xi - \xi_0)}}{(\alpha_n^- + \Gamma_n h_1/d^2)(\alpha_n^- - K_b/M_r)}. \tag{69}$$

where

$$\Lambda(\alpha_n^-, \beta_n^+) = \left[\frac{1}{2}\left(1 + \frac{K_q h}{2K_q h}\right) + \Lambda_1(\alpha_n^-, \beta_n^+) + \Lambda_2(\alpha_n^-, \beta_n^+)\right], \tag{70}$$

$$\Lambda_1(\alpha_n^-, \beta_n^+) = -\frac{\mathrm{i}\beta_a M_r}{\alpha_n^- h \beta_r}\left(1 + \frac{\alpha_n^-}{k_0'} M_x - \frac{\beta_n^+}{k_0'} M_y\right) \cos^2 K_q h, \tag{71}$$

$$\Lambda_2(\alpha_n^-, \beta_n^+) = \frac{\mathrm{i}\beta_a M_t}{2\beta_r h}\left(1 + \frac{\alpha_n^-}{k_0'} M_x - \frac{\beta_n^+}{k_0'} M_y\right)^2 \left(\frac{\sin\theta}{\alpha_n^-} - \frac{\beta_r \cos\theta}{\beta_n^+}\right) \cos^2 K_q h, \tag{72}$$

$$\alpha_n^- = -\frac{\Gamma_n h_1}{d^2} - \frac{\beta_r h_2}{d}\sqrt{K_b^2 - K_q^2 - \left(\frac{\Gamma_n}{d}\right)^2}, \tag{73}$$

$$\beta_n^+ = -\frac{\Gamma_n h_2 \beta_r}{d^2} + \frac{h_1}{d}\sqrt{K_b^2 - K_q^2 - \left(\frac{\Gamma_n}{d}\right)^2}, \tag{74}$$

$$\alpha_n^- = \frac{1}{\beta_0^2}\left[-M_x K_t - \sqrt{K_t^2 - \beta_0^2\left[(\beta_n^+)^2 + K_q^{2'}\right]}\right], \tag{75}$$

$$\beta_n^+ = -\frac{\sigma - 2\pi n}{d'}. \tag{76}$$

3. RESULTS AND DISCUSSIONS

3.1. Calculation of Eigenvalue

As indicated above, the eigenvalues will be given by

$$\Delta_h(\cos K_q \zeta_0) = 0. \tag{77}$$

For soft walls with rotor blade rows, equation (77) can be derived as

$$\left(\frac{K_q'}{k_0'}\right) \tan\, k_0' H\left(\frac{K_q'}{k_0'}\right) = \mathrm{i}\beta_a\left(1 + \frac{\alpha'}{k_0'} M_x - \frac{\beta'}{k_0'} M_y\right)^2. \tag{78}$$

One considers the eigenvalue K_q'/k_0' to be a function of some parameter, η_z. Assume β_a to be function of this parameter. If equation (78) is differentiated with respect to η_z and combined, then the following single ordinary differential equation results:

$$\frac{\partial}{\partial \eta_z}\left(\frac{K_q'}{k_0'}\right) = \frac{\mathrm{i}\beta_{af}[1 + \alpha'/k_0' M_x - \beta'/k_0' M_y]^2}{A_{ts} + 2\mathrm{i}\beta_a(\eta_z)[1 + \alpha'/k_0' M_x - \beta'/k_0' M_y]A_p}, \tag{79}$$

where

$$A_p = \frac{\pm M_x(K_q'/k_0')}{\sqrt{(K_t/k_0')^2 - \beta_0^2\left[(\beta' k_0')^2 + (K_q' k_0')^2\right]}}, \tag{80}$$

$$A_{ts} = \left[\tan k_0' H\left(\frac{K_q'}{k_0'}\right) + k_0' H\left(\frac{K_q'}{k_0'}\right) \sec^2 k_0' H\left(\frac{K_q'}{k_0'}\right)\right]. \tag{81}$$

On the other hand, the above equations have used the expression $\beta_a(\eta_z) = \eta_z \beta_{af}$, $0 < \eta_z < 1$. Therefore, if equation (79) is integrated on $0 < \eta_z < 1$, a hard-wall eigenvalue being used as the initial value, then at $\eta_z = 1$ the solution to equation (79) will be an eigenvalue for the condition β_{af}.

3.2. Solution of Integral Equation

The integral equation (44) can be reduced to a set of algebraic equations for the unknowns $f(\xi_0, \zeta_0)$. Any standard matrix package that handles equations with complex coefficients can be used to solve these equations.

3.3. Comparison with Eversman's Eigenvalues

As has been mentioned earlier that the boundary condition of a nonrigid wall takes effect on the flow field or acoustic field theoretically by the variation of eigenvalues; therefore, how to obtain accurate eigenvalues will be of particular value and theoretical importance. As a special case of solving the present eigenvalue equation, Table 1 gives the comparison between Eversman's results and that from present program under the same conditions. As shown in the table, the results agree with each other very well.

3.4. Comparison with Compressible Results with Hard Walls

When the wall admittance tends to zero, one of the theoretical results in the present analysis is the upwash velocity integral equation for the hard wall with kernel function given by equations (57) and (69). On the other hand, it is noted that the radial standing wave will have no contribution to the integration of blade pressure distribution. So, under such condition, it can be concluded that the result of solving three-dimensional integral equation for a hard wall will be the same as that from the two-dimensional model if the

TABLE 1
Calculation of eigenvalues

Mode	Starting value $\frac{\alpha}{k_0}$	Eigenvalue[1] $\frac{\alpha}{k_0}$	Eigenvalue[2] $\frac{\alpha}{k_0}$
1^+	0·0 + i0·0	1·142 + i0·217	1·1416 + i0·2170
1^-	0·0 + i0·0	0·523 + i0·353	0·5225 + i0·3526
2^+	π + i0·0	4·158 − i0·781	4·1580 − i0·7814
2^-	π + i0·0	2·388 + i0·312	2·3881 + i0·3117
3^+	2π + i0·0	4·306 − i1·955	4·3060 − i1·9551
3^-	2π + i0·0	5·243 − i0·081	5·2433 − i0·0805
4^+	3π + i0·0	7·857 − i0·478	7·8572 − i0·4778
4^-	3π + i0·0	8·214 − i0·165	8·2136 − i0·1650
5^+	4π + i0·0	11·046 − i0·326	11·0456 − i0·3264
5^-	4π + i0·0	11·248 − i0·170	11·2485 − i0·1702
6^+	5π + i0·0	14·195 − i0·248	14·1954 − i0·2481
6^-	5π + i0·0	14·326 − i0·156	14·3256 − i0·1561
7^+	6π + i0·0	17·336 − i0·200	17·3365 − i0·1998
7^-	6π + i0·0	17·427 − i0·140	17·4265 − i0·1396
8^+	7π + i0·0	20·475 − i0·167	20·4752 − i0·1671
8^-	7π + i0·0	20·541 − i0·125	20·5409 − i0·1247
9^+	8π + i0·0	23·613 − i0·144	23·6133 − i0·1435
9^-	8π + i0·0	23·663 − i0·112	23·6632 − i0·1120
10^+	9π + i0·0	26·751 − i0·126	26·7515 − i0·1257
10^-	9π + i0·0	26·791 − i0·101	26·7906 − i0·1014

[1] The results from Eversman (1977)
[2] The results from the present program.
Note: The corresponding parameters are $M_x = -0{\cdot}5, M_y = 0, \Gamma_n = 0, k_0 H = 1{\cdot}0, \beta_a = 0{\cdot}72 - \text{i}0{\cdot}42$, respectively.

blade lift and moment coefficients are defined as

$$C_{Fq} = \frac{1}{\rho_0 U_r \bar{v}_b H b} \int_0^1 \int_0^\pi \Delta\bar{p}(\xi_0, \zeta_0)\, \mathrm{d}\xi_0\, \mathrm{d}\zeta_0, \tag{82}$$

$$C_{Mq} = \frac{1}{\rho_0 U_r \bar{v}_b H b^2} \int_0^1 \int_0^\pi \xi_0 \Delta\bar{p}(\xi_0, \zeta_0)\, \mathrm{d}\xi_0\, \mathrm{d}\zeta_0, \tag{83}$$

for a bending vibration, and

$$C_{F\alpha} = \frac{1}{\rho_0 U_r^2 \alpha_t H b} \int_0^1 \int_0^\pi \Delta\bar{p}(\xi_0, \zeta_0)\, \mathrm{d}\xi_0\, \mathrm{d}\zeta_0, \tag{84}$$

$$C_{M\alpha} = \frac{1}{\rho_0 U_r^2 \alpha_t H b^2} \int_0^1 \int_0^\pi \xi_0 \Delta\bar{p}(\xi_0, \zeta_0)\, \mathrm{d}\xi_0\, \mathrm{d}\zeta_0 \tag{85}$$

for a torsional vibration, where $\bar{v}_b$ represents the amplitude of upwash velocity due to bending vibration, while α_t is the amplitude of the angular displacement due to torsional vibration of a blade.

According to the above definition Table 2 gives the results of solving the present three-dimensional integral equation and those from Smith (1972), which shows very good agreement between each other.

TABLE 2

Lift and moment coefficients

λ	Bending		Torsion	
	C_{Fq}	C_{Mq}	$C_{F\alpha}$	$C_{M\alpha}$
1·0	−0·7191 + i0·0672	0·1509 − i0·1405	−0·8236 − i0·0840	0·1824 − i0·1483
	−0·7190 + i0·0670	0·1511 − i0·1405	−0·8235 − i0·0838	0·1825 − i0·1482
1·2	−0·7502 + i0·0960	0·1328 − i0·1288	−0·9048 − i0·0634	0·1734 − i0·1934
	−0·7500 + i0·0957	0·1329 − i0·1287	−0·9044 − i0·0636	0·1735 − i0·1932
1·4	−0·3470 + i0·4620	−0·0269 − i0·1198	−0·5147 − i0·4997	−0·0257 − i0·2328
	−0·3473 + i0·4618	−0·0267 − i0·1199	−0·5149 − i0·4992	−0·0253 − i0·2327

Notes: The first row gives results from Smith (1972) for agiven reduced frequency λ, the second row is the results of the present program· Also, $\theta = 0, \sigma = \pi, M_r = 0{\cdot}5$, space/chord = 3·8.

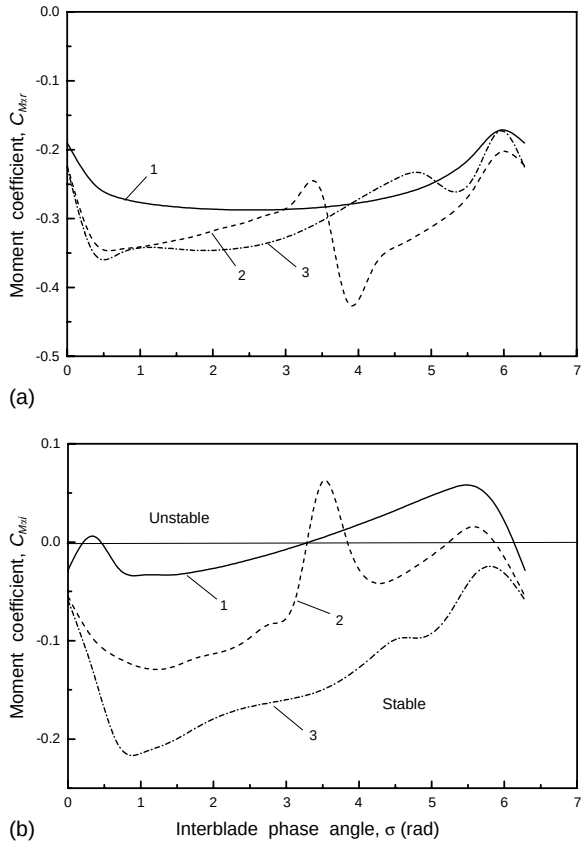

Figure 2. Effect of interblade phase angle on the moment coefficient due to torsional motion under various wall admittances: 1. hard wall; 2. soft wall, $\beta_a = (0{\cdot}15, -0{\cdot}09)$; 3. soft wall, $\beta_a = (0{\cdot}35, 0{\cdot}10)$. Besides, $\lambda = 0{\cdot}1$, $\theta = 35^\circ$, space/chord = 3·8, span/chord = 4·0, $M_r = 0{\cdot}5$. These coefficients are referred to an axis position at the leading edge point.

3.5. NUMERICAL RESULTS FOR A STATOR BLADE ROW

The moment and lift coefficients are plotted as a function of interblade phase angle in Figures 2 and 3. Perhaps the most striking feature of these plots is that the change of wall admittance will lead to a very prominent effect on both the moment and lift coefficients,

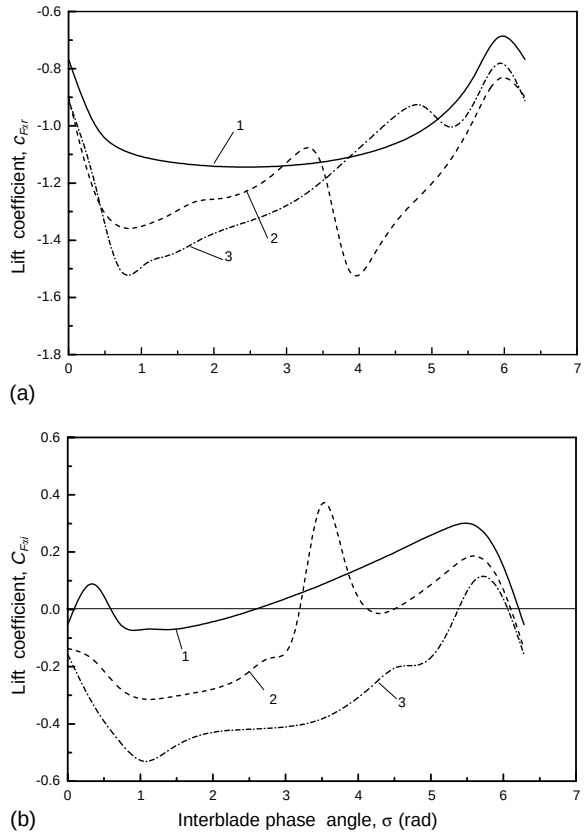

Figure 3. Effect of interblade phase angle on the lift coefficient due to torsional motion under various wall admittances. The other conditions are the same as in Figure 2.

compared with the results for hard walls. Furthermore, it is well known that the imaginary part of the moment coefficient $C_{M\alpha i}$ will determine whether the blade flutters or not, i.e. if $C_{M\alpha i}<0$, the system is stable, otherwise it is unstable. Figure 2(b) shows the effect of interblade phase angle on the aeroelastic stability of a given blade row under various wall admittance. In particular, note that for a hard wall case plotted in a solid line the blade is unstable when the interblade phase angle ranges between π and 2π, while the blade can become stable in all the range of interblade phase angles from 0 to 2π by letting the wall admittance β_a have the value (0·30,0·10). However the blade may become more unstable for $\beta_a = (0{\cdot}15, -0{\cdot}09)$ if the interblade phase angle takes value around $\sigma = 3{\cdot}1$. Therefore, from the point of view for stabilizing the blade, on the one hand, Figure 2 has actually shown that the soft wall has a positive effect on the stability for the given conditions. On the other hand, it also shows the possibility of reducing the aeroelastic stability for some wall admittance condition.

Note that Figure 2(b) indicates that the most unstable point corresponds to the interblade phase angle $\sigma = 5{\cdot}58$, which has its maximum positive moment coefficient $C_{M\alpha i} = 0{\cdot}0573$. It may be important to know how this critical point responds to the wall admittance. In fact, Figures 4 and 5 give more detailed information about the variation of the lift and moment coefficients with wall admittance. In these two plots, the wall admittance is expressed by its absolute value and argument; the latter is taken as the

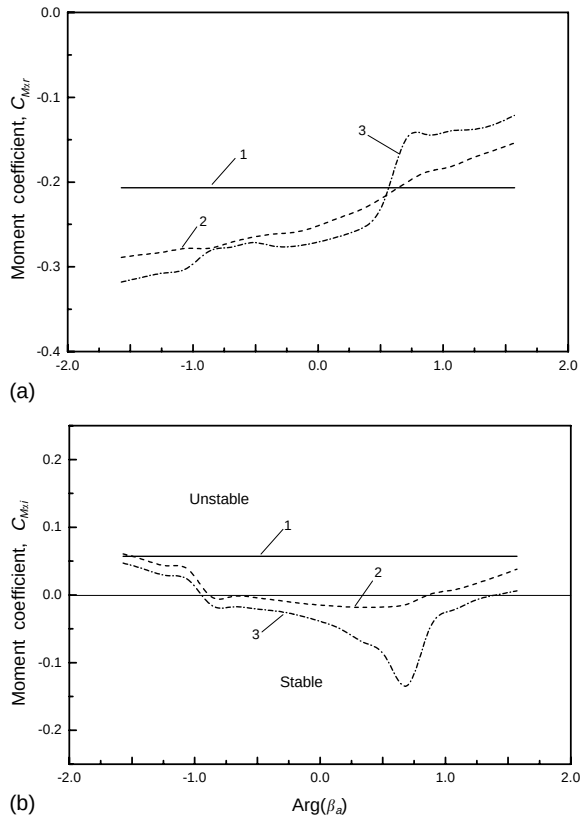

Figure 4. Variation of moment coefficient due to torsional motion with wall admittance: 1. hard wall, $|\beta_a| = 0$, 2; soft wall, $|\beta_a| = 0{\cdot}2$; 3. soft wall $|\beta_a| = 0{\cdot}5$. Besides, $\sigma = 5{\cdot}58$, $\lambda = 0{\cdot}1$, $\theta = 35$, space/chord = 3·8, span/chord = 4·0, $M_r = 0{\cdot}5$. These coefficients are referred to an axis position at the leading-edge point.

independent variable for the x-axis. It is found that for both $|\beta_a| = 0{\cdot}3$ and $|\beta_a| = 0{\cdot}5$, $C_{M\alpha i}$ is less than that for the hard wall case. In spite of this, the blade will still remain unstable when the argument varies from $-1{\cdot}57$ to $-1{\cdot}0$. However, it can be found that there are some points which enable the blade to be stable between $-1{\cdot}0$ to $1{\cdot}0$. These results illustrate that a soft wall can have a positive or negative effect on suppressing blade flutter, depending on the admittance value that the wall possesses.

3.6. Numerical Results for a Rotor Blade-Row

As indicated above, if the incoming velocity U_r along the chordwise direction and other geometrical conditions remain the same, the upwash integral equation for both a stator blade-row and a rotor blade-row with a hard wall will have the same expression. However, for a soft wall their integral equations will have differences in two aspects. First, there is an additional term for the expression of kernel function of a rotor blade-row, which is related to the circumferential Mach number M_t of the blade. Second, the transformation between a duct-fixed coordinate and a blade-fixed coordinate will lead to the shift of perturbation frequency of the blade; this means that the real frequency interacting with the wall will be different from that for a stator blade row. In fact, it can be

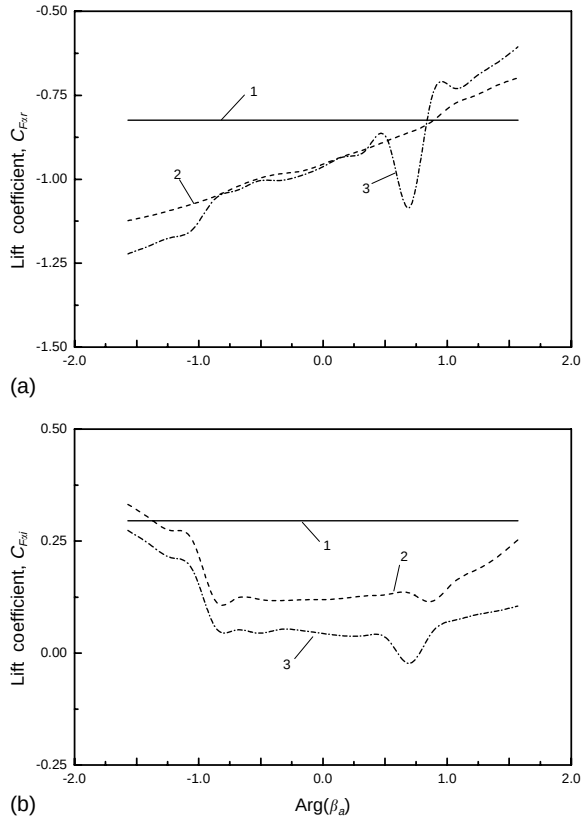

Figure 5. Variation of lift coefficient due to torsional motion with wall admittance. The other conditions are the same as in Figure 4.

shown from equation (64) that,

$$\omega_t = \omega_b + B_r(\sigma' - n)\Omega, \quad n = 0, \pm 1, \pm 2, \ \ldots, \tag{86}$$

where $\sigma' = \sigma/2\pi$ and B_r is the blade number of the rotor.

Equation (86) shows that the frequency in a duct-fixed coordinate not only depends on the speed of rotor Ω but the interblade phase angle σ. Perhaps the more important feature from this expression is that for a stator blade-row where all modes interact with the wall in the same frequency, while for a rotor blade-row each mode has its own frequency which corresponds to different mode number n shown in equation (86). Hence, for a rotor blade-row, it will be unreasonable to assume that the wall has the same admittance for all modes. This actually means that, if one hopes to control the aeroelastic stability of a given blade row through the wall, it must be designed to have required frequency response for each mode, at least for some principal modes, to affect the blade aerodynamic loading. As a theoretical analysis, Figures 6 and 7 give the results under the assumption that, if circumferential mode number $|n| < 10$, β_a has a given value, otherwise $\beta_a = 0$. These plots clearly indicate that even though a few modes are controlled through the wall, it can be still found that the lift, moment coefficients and the stability of the blade will all be changed prominently compared with the results for the hard wall case.

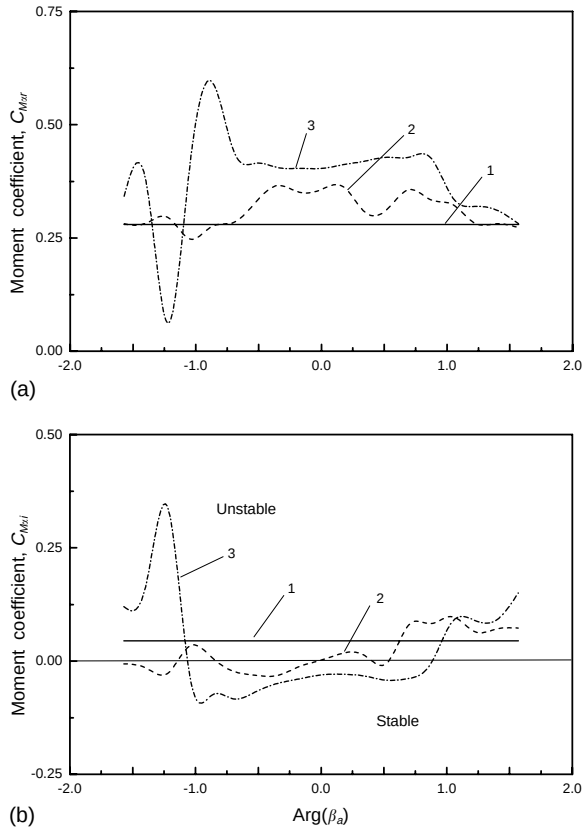

Figure 6. Variation of moment coefficient due to torsional motion with wall admittance: 1. hard wall, $|\beta_a| = 0$; 2. soft wall, $|\beta_a| = 0{\cdot}6$; 3. soft wall $|\beta_a| = 1{\cdot}2$. Besides, $\sigma = 1{\cdot}04$, $\lambda = 0{\cdot}05$, $\theta = 35$, space/chord = 3·8, span/chord = 4·0, $M_r = 0{\cdot}5$, $M_t = 0{\cdot}57$. These coefficients are referred to an axis position at the mid-chord point.

4. CONCLUDING REMARKS

As has been discussed in the Introduction, control of blade flutter by use of a nonrigid wall has several advantages compared with the existing method of suppressing blade flutter. But it leads to numerous theoretical problems which have never been clearly elucidated by the existing theories. In fact, control of flow by changing the wall boundary condition is a typical three-dimensional problem. So, a three-dimensional aerodynamic model describing the physical process will inevitably be required. However, it can be verified that the eigenfunctions of a duct system containing mean flow will not satisfy the orthogonality property under a nonrigid wall boundary condition. Besides, an important fact is that the existing lifting surface theories for unsteady aerodynamics and aeroacoustics of turbomachines are all based on the assumption of a rigid boundary condition, which has unitized the orthogonality of eigenfunctions. This means that, in principle, the existing models cannot be used directly to treat a nonrigid boundary problem. So, how to set up a new lifting surface model under a nonrigid wall boundary condition will be of particular importance. In the present investigation, a new lifting surface model has been suggested based on the application of generalized Green's function theory and double Fourier transformation technique, which is expressed as various upwash integral equations and the corresponding kernel function. It is found that the change of wall boundary condition not

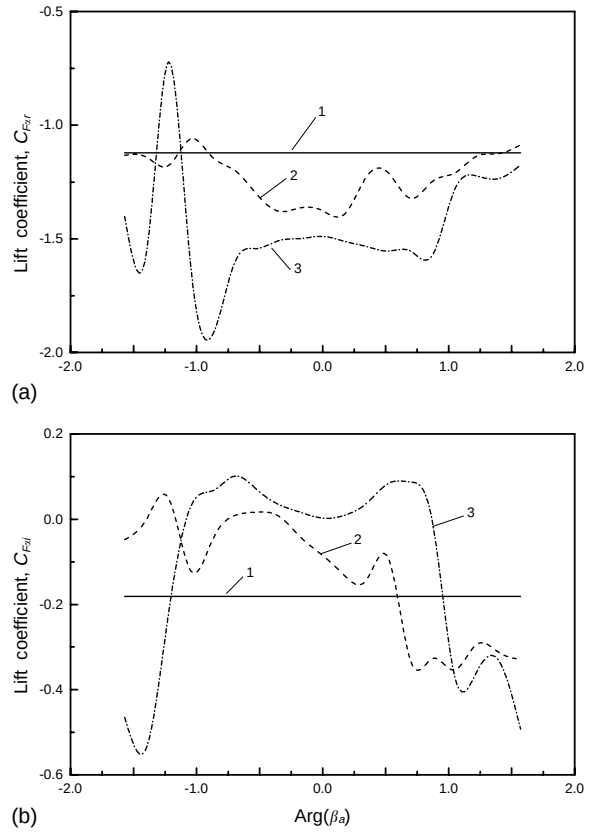

Figure 7. Variation of lift coefficient due to torsional motion with wall admittance. The other conditions are the same as in Figure 6.

only affects the eigenvalues of the system but also the eigenfunction normalizing factor in comparison with a rigid boundary condition, and it is these variations that finally affect the flow and acoustic field. On the other hand, it is noted that under a nonrigid boundary condition the kernel function expression for a rotor blade-row is different from that for a stator blade-row due to the motion and boundary condition effect, while under a rigid boundary condition these expressions can be reduced to the same results as those given in the previous lifting surface models.

Calculation of eigenvalues is another important link for a nonrigid boundary problem. In the present analysis, various eigenvalue equations have been derived under a given geometrical condition, and then transformed into an ordinary equation with the eigenvalue of a rigid wall as its initial value.

Numerical simulation consists of three parts in the present investigation. In the first part, calculation of eigenvalues under a given wall admittance value is checked, which is in agreement with the existing results. A special case of the present lifting surface model is equivalent to the existing theory for a rigid boundary condition. This provides further means for checking the theoretical results. In fact, the moment and lift coefficients calculated by the present program show good agreement with those available in literature. Based on this verification, the calculation is then extended to study the effect of a nonrigid wall on the flow of a stator and rotor blade-row. It is found that the change of wall admittance will lead to a remarkable effect on both lift and moment coefficients. Perhaps

the most important conclusion drawn from the present investigation is that whether a nonrigid wall has positive or negative effect on suppressing blade flutter will mainly depend on what admittance value the wall possesses. This conclusion has two additional implications. First, it is possible to design a liner for suppressing blade flutter. Second, while modern commercial jet engines all use the nonrigid wall or liner to suppress the noise, the intrinsic frequency of the liner falls into the same frequency band as that due to the vibration from a rotor blade-row, which is measured in a duct-fixed coordinate system. Thus, the present analysis suggests that the frequency placement of the liner can have a negative effect on the aeroelastic stability. This situation can be remedied at the design stage.

ACKNOWLEDGMENTS

The work described here was carried out while one author (X. Sun) was supported by an JSPS Fellowship. The authors are indebted to Prof. T. Watanabe from the University of Tokyo for many helpful discussions.

REFERENCES

BECHERT, D. W. 1980 Sound absorption caused by vorticity shedding, demonstrated with a jet flow. *Journal of Sound and Vibration* **70,** 389–405.

BENDIKSEN, O. O. 1988 Recent developments in flutter suppression techniques for turbomachinery rotors. *Journal of Propulsion and Power* **4,** 164–171.

BENDIKSEN, O. O. 1993 Aeroelastic problems in turbomachines. In *Flight Vehicle Materials, Structures and Dynamics-Assessment and Future Directions* (eds A. K. NOOR & S. L. VENNERI), Vol.5, Chapter 3, pp. 241–297. New York: ASME.

BREKHOVSKIKH, L. M. 1960 *Waves in Layered Media*. New York: Academic Press.

DOWLING, A. P. & HUGHES, I. J. 1992 Sound absorption by a screen with regular array of slits. *Journal of Sound and Vibration* **156,** 387–405.

EVERSMAN, W. 1975 Computation of axial and transverse wave numbers for uniform two-dimensional ducts with flow using a numerical integration scheme. *Journal of Sound and Vibration* **41,** 252–255.

EVERSMAN, W. 1977 Initial values for the integration scheme to compute the eigenvalues for propagation in ducts. *Journal of Sound and Vibration* **50,** 159–162.

GOLDSTEIN, M. 1976 *Aeroacoustics*. New York: McGraw-Hill.

HOWE, M. S. 1979*a* Attenuation of sound in a low Mach number nozzle flow. *Journal of Fluid Mechanics* **91,** 209–229.

HOWE, M. S. 1979*b* On the theory of unsteady high Reynolds number flow through a circular aperture. *Proceedings of the Royal Society* (London) A **366,** 205–223.

HUGHES, I. J. & DOWLING, A. P. 1990 The absorption of sound by perforated linings. *Journal of Fluid Mechanics* **218,** 299–335.

JING, X. & SUN, X. 1999 An experimental investigations of perforated liner with bias flow. *Journal of the Acoustical Society of America* **106,** 2436–2441.

KO, S.-H. 1973 Sound attenuation in acoustically lined circular ducts in the presence of uniform flow and shear flow. *Journal of Sound and Vibration* **22,** 193–210.

LORDI, J. A. & HOMICZ, G. F. 1981 Linearized analysis of the three-dimensional compressible flow through a rotating annular blade-row. *Journal of Fluid Mechanics* **103,** 413–442.

MARSHALL, J. G. & IMREGUN, M. 1996 A review of aeroelasticity methods with emphasis on turbomachinery applications. *Journal of Fluids and Structures* **10,** 237–267.

MORSE, P. M. & FESHBACH, H. 1953 Methods of Theoretical Physics, Vol. 1, pp. 791–895. New York: McGraw-Hill.

NAMBA, M. YAMSAKI, N. & KURIHARA, Y. 1984 Some three-dimensional effects on unsteady aerodynamic forces on oscillating cascades. *Proceedings Third International Symposium on Aeroelasticity in Turbomachines*, pp. 217–230.

NAMBA, M & FUKUSHIGE, K. 1982 Application of the equivalent surface source method to the acoustics of duct systems with non-uniform wall impedance. *Journal of Sound and Vibration* **73,** 125–146.

NAMBA, M. 1977 Three-dimensional analysis of blade force and sound generation for an annular cascade in distorted flow. *Journal of Sound and Vibration* **50,** 479–508.
RIENSTRA, S. W. 1986 Hydrodynamic instabilities and surface waves in a flow over an impedance wall. *Aero- and Hydro-acoustics*, *IUTAM Symposium*, Lyon, 1985, eds. G. Come-Bellot, & J. E. Ffowcs Williams, pp. 483–490. Berlin: Springer-Verlag.
SCHULTEN, J. B. H. M. 1984 Vane stagger angle and camber effects in fan noise generation. *AIAA Journal* **22,** 1071–1079.
SIJTSMA, P. 1995 Prevention of buzz-saw noise by acoustic lining. CEAS/AIAA-Paper 95-077, pp. 575–583.
SMITH, S. N. 1972 Discrete frequency sound generation in axial flow turbomachines. *ARC Reports and Memoranda*, No. 3709.
TESTER, B. J. 1972 The propagation and attenuation of sound in lined ducts containing uniform or "plug" flow. *Journal of Sound and Vibration* **28,** 151–203.
VENTRES, C. S., THEOBALD, M. A. & MARK, W. D. 1983 Turbofan noise generation. NASA CR-167952, Vol. I.
WATANABE, T. & KAJI, S. 1984 Possibility of cascade flutter suppression by use of nonrigid duct wall. *Proceedings Third International Symposium on Aeroelasticity in Turobomachines*, pp. 261–276.
WHITEHEAD, D.S. 1960 Force and moment coefficients for vibrating aerofoils in cascade. *ARC Reports and Memoranda* No. 3254.
ZHAO, H. & SUN, X. 1999 Active control of wall acoustic impedance. *AIAA Journal* **37,** 825–831.
ZORUMSKI, W.E. 1974 Acoustic theory of axisymmetric multisectioned ducts. NASA TR R-419.

APPENDIX: NOMENCLATURE

b	blade semichord
h	height from the hub to the tip side in the transformed space
h_1	stagger distance, measured parallel to chord
h_2	gap distance, measured normal to chord
i	$\sqrt{-1}$
k_b	wave number, $k_b = \omega_b/a_0$
$\bar{p}_m$	amplitude of perturbation pressure for mth blade
$\bar{v}$	upwash velocity of the reference blade
x, y, z	a blade-fixed coordinate system for an observer
x_0, y_0, z_0	a blade-fixed coordinate system for a source
x', y', z'	a duct-fixed coordinate system
t	time in an observer point
A_b	the upper or lower surface of a blade
A_{ab}	periphery of a blade
$C_{Fqi}, C_{F\alpha i}$	imaginary part of blade lift coefficient
$C_{Fqr}, C_{F\alpha i}$	real part of blade lift coefficient
$C_{Mqi}, C_{M\alpha i}$	imaginary part of blade moment coefficient
$C_{Mqr}, C_{M\alpha r}$	real part of blade moment coefficient
H	height from the hub to the tip side
M_x	Mach number in x'-direction
M_y	Mach number in negative y'-direction
M_t	Blade circumferential Mach number in mean radius
U_r	mean velocity in chordwise direction
V_n	normal velocity of a body boundary

Greek letters

α	wave number in ξ-direction
β	wave number in η-direction

β_a	wall admittance
η_z	independent variable of wall admittance
η_{0m}	source coordinate for the mth blade
θ	blade stagger angle
λ	reduced frequency based on blade chord
$\Lambda_h, \Lambda_s, \Lambda_v$	eigenfunction normalizing factor
ξ, η, ζ	a blade-fixed coordinate system for an observer, in the transformed space
ξ_0, η_0, ζ_0	a blade-fixed coordinate system for a source, in the transformed space
ξ_p	particle displacement
ξ_{pa}	amplitude of particle displacement
ξ_{0m}	source coordinate for the mth blade
ξ_{pi}	particle displacement inside the surface of a liner
ξ_{po}	particle displacement outside the surface of a liner
ρ	perturbation density
ρ_0	mean density
σ	interblade phase angle
τ	time in a source point
ω	angular frequency
ω_b	perturbation frequency of blade force
$\Delta\bar{p}_m$	amplitude of pressure difference for the mth blade
Ω	rotating speed of rotor